M.J. Fox, N. Goldstein, P. Vujkovic-Cvijin, B. Gregor, S. Adler-Golden, J. Cline, B. St Peter, A. Lowell, and M. Wilder, A compact, thermal-infrared spectral imager for chemical-specific detection, Proc. SPIE 8870, Imaging Spectrometry XVIII, 887004 (2013).

http://dx.doi.org/10.1117/12.2024317

See next page.

A compact, thermal-infrared spectral imager for chemical-specific detection

Marsha Fox[*1], Neil Goldstein[1], Pajo Vujkovic-Cvijin[1], Brian Gregor[1], Steven Adler-Golden[1], Jason Cline[1], Benjamin St Peter[1], Augustus Lowell[2], and Mark Wilder[2]
[1]Spectral Sciences, Inc., 4 Fourth Ave. Burlington MA, 01803
[2]Triple Ring Technologies, Beverly MA, 01915

ABSTRACT

A second-generation long-wave hyperspectral imager based on micro-electro-mechanical systems (MEMS) technology is in development. Spectral and spatial encoding using a MEMS digital micro-mirror device enables fast, multiplexed data acquisition with arbitrary spectral response functions. The imager may be programmed to acquire spectrally selective contrast imagery, replacing more time-consuming hyperspectral data collection. A single-element detector collects encoded data and embedded real-time hardware generates imagery. An internal scanning mechanism enables rapid retrieval of full hyperspectral imagery. The resulting rugged, low-cost sensor will provide chemically specific imagery for applications in gaseous and surface contaminant detection, surveillance, remote sensing, and process control.

1. INTRODUCTION

A second-generation, micro-electro-mechanical systems (MEMS)-based, hyperspectral imager will extend the previously developed Adaptive Multiplexing Spectrometer (AMS) [1,2] breadboard into a compact, fully integrated fieldable unit. The system is called the Thermal infrared, Reconfigurable, Analysis Camera for Explosive Residue (TRACER) after its first planned application. The system will produce hyperspectral imagery and chemical-specific thermal infrared contrast imagery for visualization, detection, and quantification of chemical species through their characteristic long-wave infrared spectral signatures. The spectrometer uses a set of concave gratings, a MEMS digital micro-mirror device (DMD), and a single-pixel Stirling-cooled detector to produce spectrally selective scene imagery. The instantaneous field-of-view includes a spectral and one spatial dimension. The image field-of-view is scanned by a movable, DMD-synchronized slit at the spectrometer entrance to provide a second spatial dimension.

The sensor may operate in hyperspectral imaging mode; however its strength lies in producing hyperspectral detection filters in hardware to rapidly generate contrast imagery. This mode is accessed by implementing analog transmission functions with the DMD using grey scales. Thus linear algorithms, including traditional detection methods such as matched filters, orthogonal subspace projection, and principal component analysis, can be implemented in hardware. The firmware DMD programming will enable an operator to rapidly change operating mode and spectral, temporal and spatial resolution. For instance, the system can be programmed to operate on sub-arrays of pixels in order to more rapidly interrogate an area or collect high-resolution spectra.

2. SYSTEM DESCRIPTION

TRACER, like AMS, uses a Digital Micro-Mirror Device, (DMD) a commercially available 2D array of micro-mirrors built by Texas Instruments, and a single detector, to collect spectrally encoded image data, a process shown schematically in Figure 1. A single realization of a pattern in the DMD mirrors is referred to as a 'mask.' In TRACER, the masks will be cycled at up to the hardware limited rate of 30 kHz. The system uses a standard LWIR camera foreoptic to produce an image on the input slit of a concave-grating spectrograph, represented in the diagram for simplicity as a prism-shaped dispersive element. The spectral range is 7.5-12.5 μm. With a maximum of 64 channels, the limiting spectral resolution is FWHM=0.08 nm. The spectrograph produces a spectrally dispersed image on the DMD. The DMD processor is loaded with a sequence of binary masks (step 1 in the Figure 1) that encode spatial and spectral information by selectively passing or rejecting light of specific wavelengths. Light selected by the DMD is directed towards a second grating spectrograph that spectrally recombines the light and focuses the image onto a single detector, producing an encoded analog signal stream.

*mfox@spectral.com; phone 781 273 4770; fax 781 270-1161; www.spectral.com

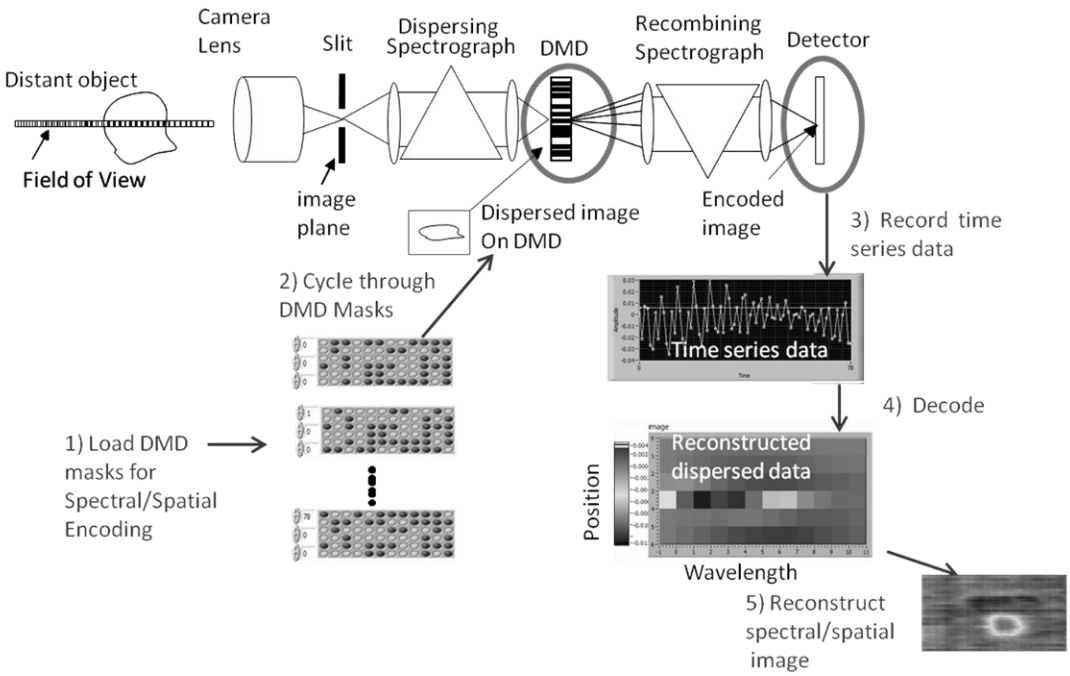

Figure 1. Schematic of sensor operation. A sequence of DMD masks encode a binary on (green) or off (grey) pattern on the image at the DMD plane. The resulting analog signal is recorded and decoded using matrix math.

The core of the AMS is the versatility provided by the DMD to encode any spatial or spectral pattern into the data stream. In standard operating mode, the data is encoded with a spectral detection filter, that discriminates a specific material of interest from backgrounds and confusor materials [2] The system software can be configured to implement any linear analog detection filter in DMD hardware and apply it to the incoming signal to produce a two dimensional detection map. The signal can alternatively be encoded to produce a hyperspectral image using Hadamard transform encoding [3], or to cycle through any series of spectral functions.

Detection images are created by using a series of encoding masks that are automatically generated on the DMD from internal spectral libraries of target materials and scene background spectra. The data processor cycles through the masks (step 2) time sequence data is collected (step 3) and decoded (step 4) to reconstruct the spectral/spatial image in near real time (step 5). Detection filters can be changed on the fly or cycled to create images of multiple target materials, or to refine the filter to discriminate against specific confuser materials that may be prominent in the local environment. The detection images, which map the location of detected materials in the scene, can then be superimposed on a wide band thermal image created with the same data.

The instantaneous field of view is 1D spatial by 1D spectral. For the previous AMS program, an external scan mirror was used to produce a second spatial dimension. However the optical design of the system can accommodate a second spatial dimension internally, by translating the slit across the image plane—along the vertical line in Figure 1. In TRACER, a scanning slit will be implemented that will synchronize with the DMD. This will increase the speed of full image acquisition while maintaining a small sensor footprint. The resolved spatial image size is typically to 80x80 pixels.

The optical layout of TRACER is shown in Figure 2. The system uses a set of f/1.8 machined gratings that are 85% efficient at the peak wavelength, a standard IR camera lens, and a Texas Instruments DMD and electronics. The DMD has been modified with a ZnSe window. The overall system efficiency is projected to be better than or equal to the 12% value obtained in the precursor AMS system. Efficiency at long wavelengths is limited due to diffraction effects from the 13 µm square micro-mirrors. Efficiency could be improved if a digital micro-mirror assembly with larger mirrors were available. The TRACER detector is a 2x2 mm HCT within a Stirling cooler. The entire optical system including Stirling cooler and slit assembly fits within a 170 mm cube, shown in Figure 2b.

The image quality of the TRACER system is illustrated with spot diagrams at the intermediate DMD plane, Figure 3a and on the detector, Figure 3b. The horizontal dimension of the image is produced at a single slit position while the vertical dimension is from successive slit scan positions. The geometric linearity of the dispersed image on the DMD is critical to successfully encoding filter and Hadamard masks. The full 2D image is formed on the square detector, as illustrated in Figure 3b, which shows the spot diagram on the detector for objects at the center, corners, and edges of the field of view.

The electronic system architecture is illustrated by the block diagram in Figure 4. The electronic systems are connected by a custom I/O adapter. The I/O adapter conditions power, provides interfaces between component controllers and monitors temperatures within and outside the sensor package. The synchronized control of the DMD pattern generation, slit-scan motor, and data acquisition is driven by custom firmware loaded onto a DLI Discovery 4100 board modified with an upgraded Xilinx FPGA. General software system operations, file handling, data processing, and the user interface are handled by a single board computer (SBC) equipped with a dual core AMD CPU and the Windows 7 Embedded Standard operating system. The SBC runs a Labview application that is built around Labview's Actor Framework, a recently introduced object oriented software library that facilitates concurrent programming, taking maximum advantage of the two cores on the SBC. Storage for target and background spectral libraries, data and meta-data is managed on the SBC using a SQL database. The SBC further controls additional hardware such as the display, video camera, and communications electronics.

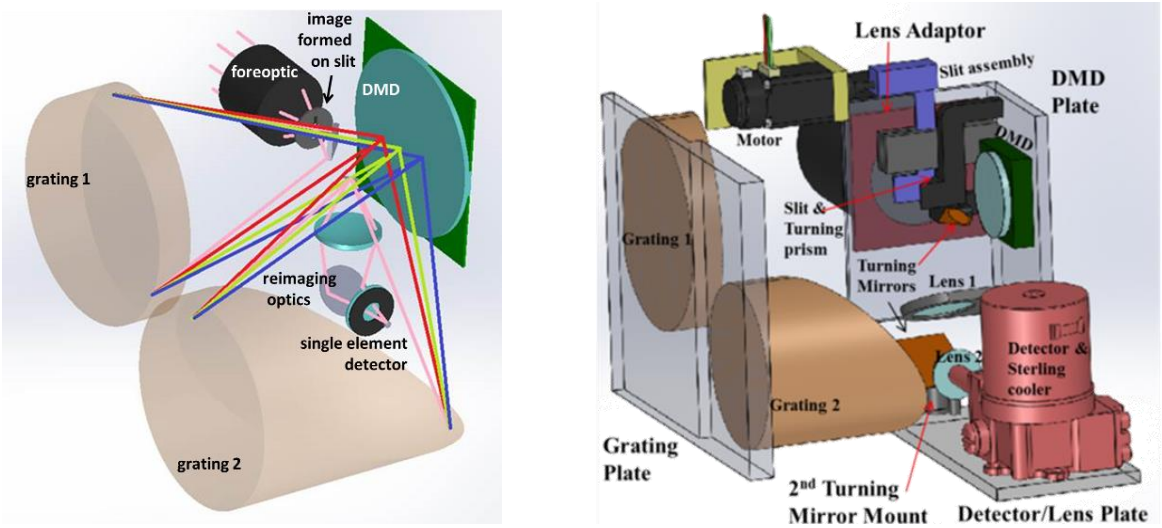

(a) **(b)**

Figure 2. TRACER Optical System a) ZEMAX layout, b) SolidWorks layout with Stirling cooled detector and scanning slit mechanical assembly.

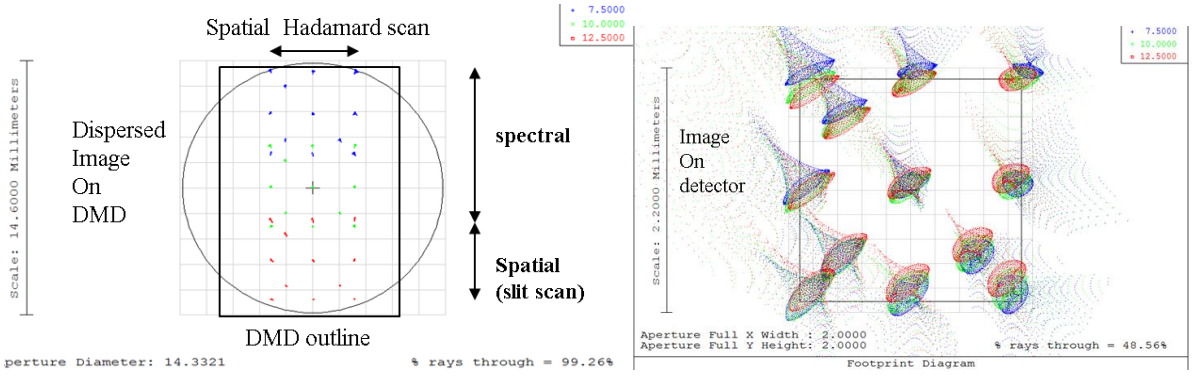

(a) **(b)**

Figure 3. Optical Quality at a) DMD and b) Detector Planes

The SBC initiates data collection by sending data structures that specify a DMD frame sequence over a USB connection to the 4100 board. The on-board FPGA is programmed with custom firmware which generates the required DMD frame sequences for Hadamard or analog filters, sends timing signals to the slit motor controller, and acquires data from the detector. Data is decoded in the Labview software on the SBC and hyperspectral or detection map images are formed.

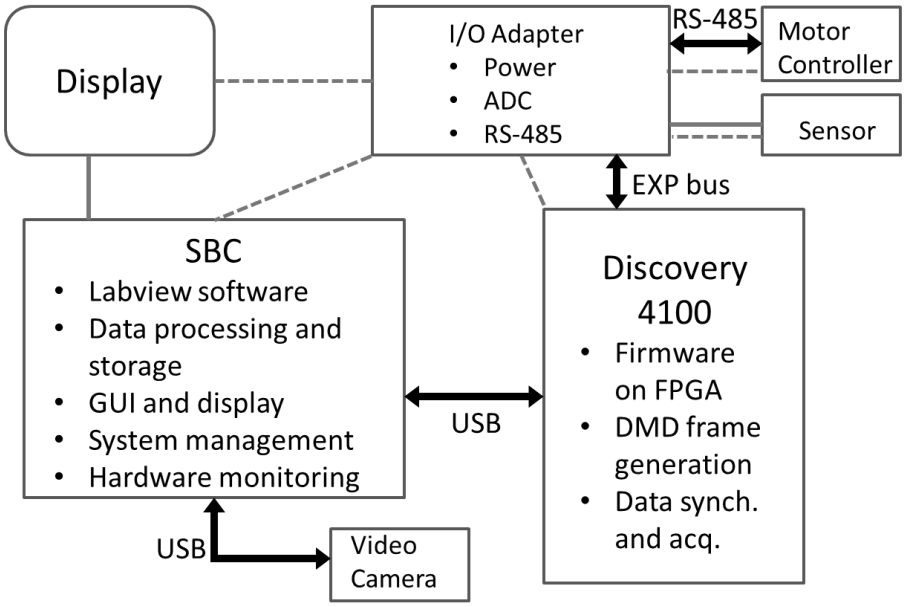

Figure 4. Electronics block diagram. The dashed lines indicate power distribution from the I/O adapter.

A preliminary layout of the full TRACER system showing optics and electronics is shown in Figure 5, with a large foreoptic 25-150mm zoom lens attachment. The width and depth are driven by the optical design, while the height was driven by the choice to use a standard DLI 4100 board for control and data acquisition, and could be substantially reduced in a third generation. The presence of an on-board SBC aides development but could be replaced by a second FPGA and firmware. The system will be self-contained and run on internal batteries or wall power.

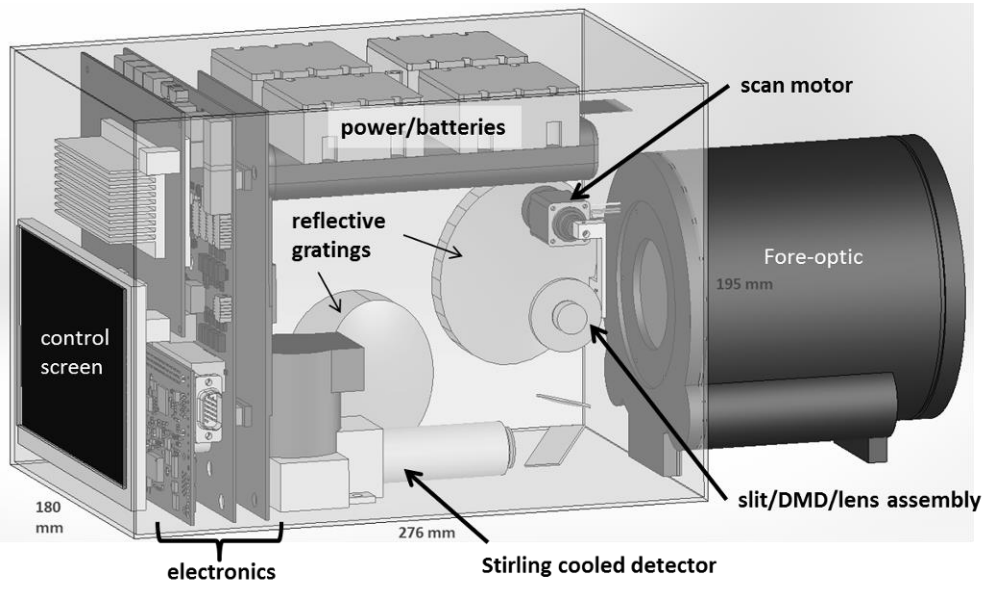

Figure 5. Preliminary Second Generation (TRACER) layout

Analog Filter Detection Algorithms

Like AMS, the system will be user selectable between collection of hyperspectral imaging and analog filter detection imaging. In operation, the system will be run primarily in detection imaging mode with known target spectra. A sequence of several filters testing for a variety of target materials or members of a target class can be acquired in a faster timeframe that it would take to collect and process a full hyperspectral image, with the advantage that each detection image is less susceptible to relative motion between the sensor and target. The current detection algorithm being tested is a generalized matched filter optimized to maximize the signal to noise expression:

$$SNR^2 = h^T s s^T h / (h^T R h + C^2(p^2+q^2)) \quad (1)$$

where h is the filter, s is the background mean-subtracted target spectrum, and R is a covariance matrix formulated from background spectra. The last term is the mean square read noise. The filter is implemented as a weighted difference between two successive masks, one for the positive parts of the filter and one for the negative, whose maximum values are unity. Thus the respective weightings are defined as 1/p and 1/q, where the larger of p and q equals 1. An Amoeba multi-dimensional minimization routine [4], based on the downhill simplex method is run to select h, p and q. The sum of the two filter masks includes signal from the full spectral range and is essentially a wide band image. In Figure 6, results from AMS, taken in 2009, show the matched filter detection of R134 gas in a HDPE bag with an external scanner to obtain the horizontal dimension. The visible image shows the same scene with and without the bag.

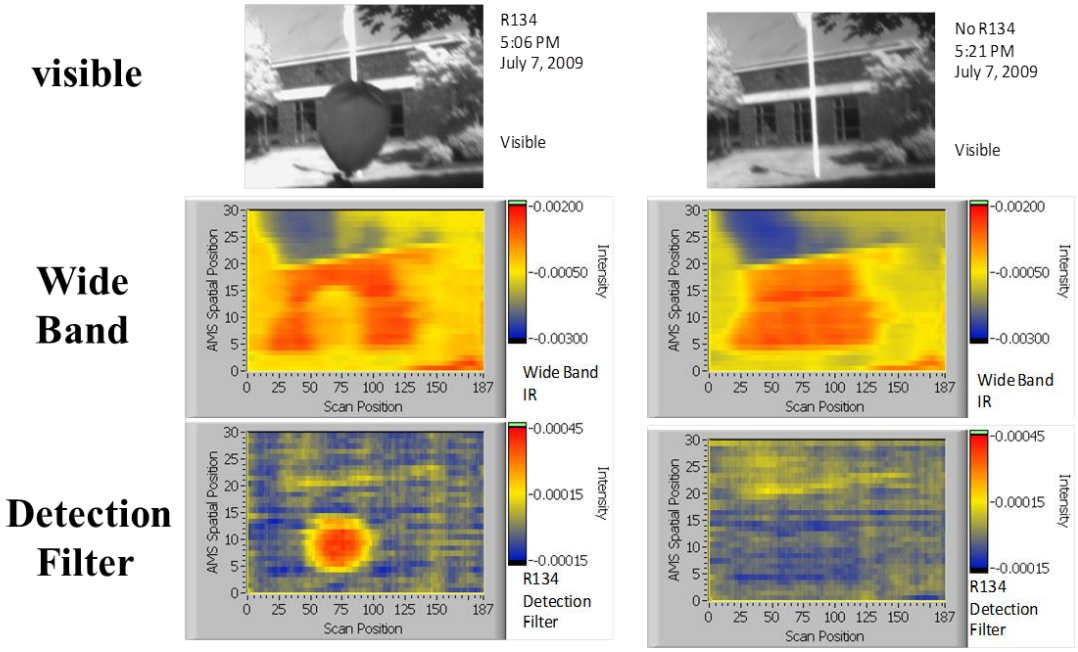

Figure 6. AMS wide band image and matched filter detection results for a R134 gas target.

Although analog filters such as the generalized matched filter are not the only way to detect materials in spectral imagery, they are widely used on hyperspectral imagery in post-processing to search for known targets. The advantages of constructing filters in hardware over post processing include a SNR advantage, as well as the reduction in data handling and storage requirements typical of hyperspectral imagery.

The improvement in SNR using a hardware matched filter is due to a reduction in the additive read noise from collecting two frames of data rather than N, where N is the number of spectral channels. To demonstrate this we calculate the SNR for the TRACER system at a single spatial pixel, when a full hyperspectral image is collected and processed with a matched filter, SNR_p, and compare it to the SNR for a hardware matched filter, SNR_h. For a system of N spectral channels, N DMD masks are required to generate a single spectrum on a single pixel. Let s_i equal the continuous signal level in a specific channel i acquired over a single mask realization time, Δt. Using the Hadamard transform method of data collection, half the N DMD mirrors are off for a given mask realization, so the signal at channel i for N masks is

$Ns_i/2$. Defining the read noise for a single mask as n, the noise for N masks is summed in quadrature: $n\sqrt{N}$. Thus the SNR of channel i for full spectrum acquisition is:

$$SNR = s_i\sqrt{N}/2n \tag{2}$$

To produce the processed matched filter response, the N matched filter values at each channel, f_i, are applied to the measured signal values and then summed:

$$s_p = \frac{N}{2}\sum_i^N f_i s_i\,, \tag{3}$$

and the processed filter noise is

$$n_p = n\sqrt{N}\sqrt{\sum_i^N f_i}\ . \tag{4}$$

The hardware matched filter acquisition is made using a single pair of N-mirror masks that can be held in position for multiples, m, of Δt. By analogy with Equation 3 the summed hardware matched filter signal is

$$s_h = \frac{m}{2}\sum_i^N f_i s_i\,, \tag{5}$$

Using the weightings p and q obtained from filter optimization, as described in Equation 1, and applying them to the positive and negative filter outputs, the noise in each mask is multiplied by p or q, integrated over time $m\Delta t/2$, and summed over the mask pair in quadrature, yielding

$$n_h = n\sqrt{m\left(p^2+q^2\right)/2}\,, \text{ and} \tag{6}$$

$$SNR_h = \frac{\sqrt{m}\sum_i^N f_i s_i}{n\sqrt{2\left(p^2+q^2\right)}} \tag{7}$$

Note that for noisy data acquisition p and q are similar in size and around twice the typical average matched filter values f_i, so we can make the approximation:

$$n_p \cong 0.5nN\sqrt{\left(p^2+q^2\right)/2} \tag{8}$$

$$SNR_p \cong \frac{\sqrt{2}\sum_i^N f_i s_i}{n\sqrt{\left(p^2+q^2\right)}}\,, \text{ and} \tag{9}$$

$$SNR_h \cong \frac{\sqrt{m}}{2}SNR_p\,. \tag{10}$$

Thus for a given filter, the hardware version can yield a significant improvement in SNR over the processed, in a fraction of the acquisition time, regardless of the spectral resolution. If the hardware matched filter were used to acquire a detection image in the same time as the full 64 channel spectral image (m=N=64), the SNR advantage would be a factor of 4. More likely, the matched filter would be acquired in a much shorter time frame, and multiple target filters would be obtained with the hardware filter. The hardware and processed SNRs are equal when m=4, in which case 16 different target filters could be applied in the time $N\Delta t$ that it would take to collect a single hyperspectral cube for processing.

In practice, the TRACER matched filters will be formulated from an internal library of known target spectra. Background spectra may not be known and are preferably obtained locally, although a library of global background material spectra, including manmade materials such as car paints will be stored. New backgrounds will be acquired by operating in full hyperspectral imaging mode using a Hadamard sequence, selected by the user and stored in libraries on the SBC. The effects of the changing atmosphere and surface temperature on filter effectiveness for rejection of non-target materials are being investigated.

Preliminary Testing

The AMS system was originally designed and demonstrated for chemical gas detection [2] as illustrated in Figure 6. TRACER is initially intended for detection of solids at low levels on surfaces. We are using the AMS to take preliminary measurements and develop filter algorithms. TRACER is intended for outdoor use and performs best using sky illumination with the target surface at approximately 45º angle from zenith and the optical axis. In Figure 7, a simple laboratory setup has been used to illuminate the test surface with similar contrast to the out door scenario. The sample is illuminated with a hot blackbody using a gold-coated 45 degree flat mirror.

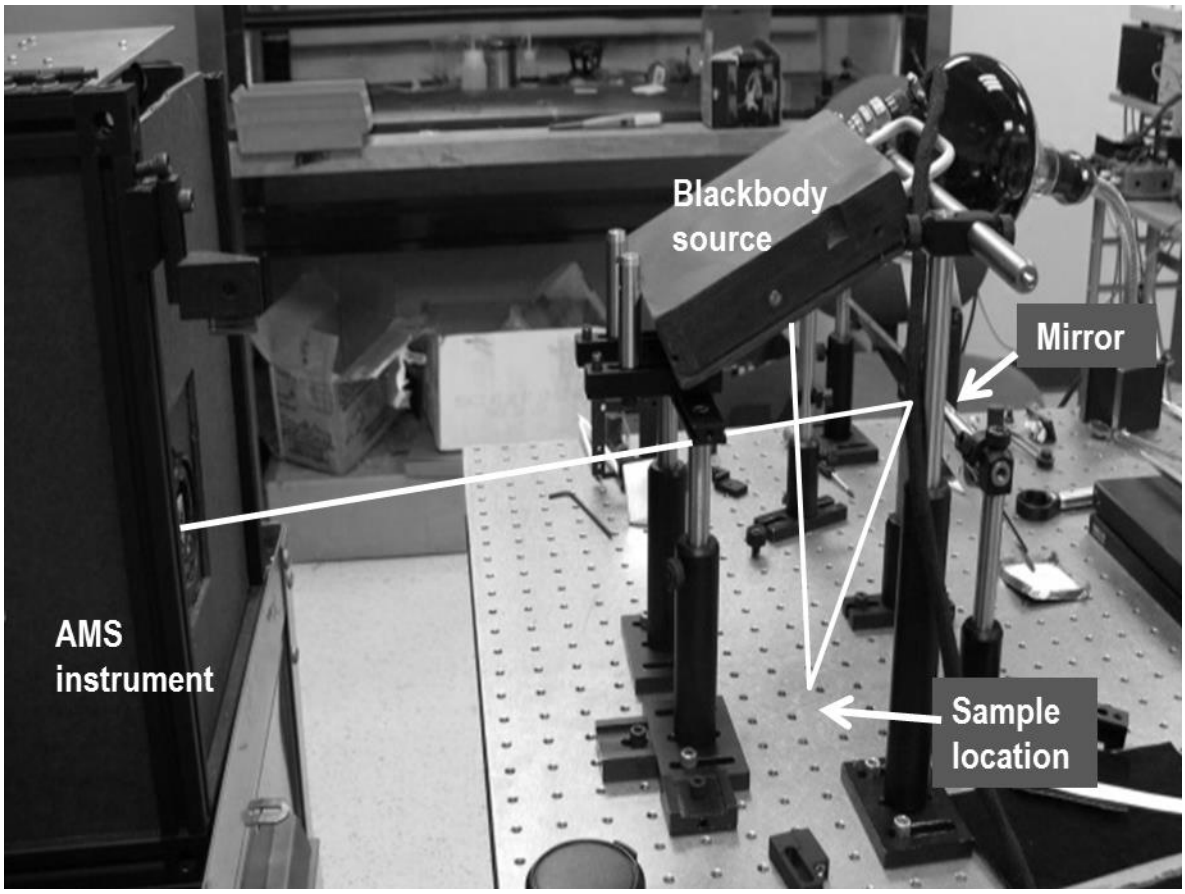

Figure 7. Simple lab test setup

Spectra of finely ground potassium nitrate (KNO_3) powder were obtained using the AMS system and compared to FTIR measurements. Spectral features were verified, although the AMS instrument function for this measurement series was too low at 11 microns to observe the feature there. A matched filter was formed using the KNO_3 spectrum and blackbody radiance spectrum as background. The powder was contained in a tray in the center of the image area. The matched filter was applied to six spatial channels at a single slit position that spanned the image area. The spectra and filter results are shown in Figure 8. The matched filter response is high in the central three spatial channels, which were completely or partially filled with KNO_3.

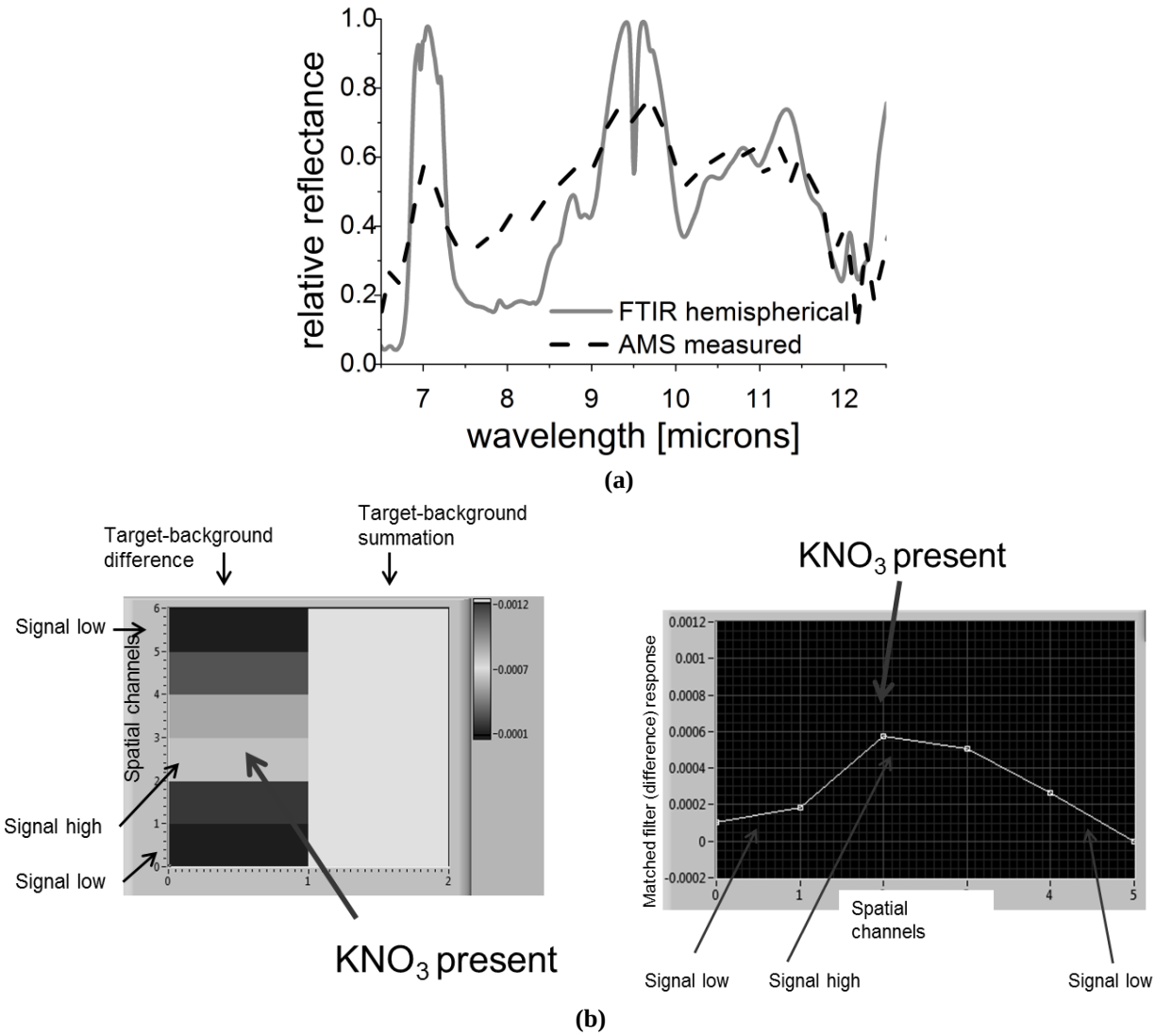

Figure 8. Measurement of bulk potassium nitrate. a) Measured spectra showing features at 7 microns and between 9 and 10 microns, FTIR spectrum provided by T. Blake, PNNL, 2013. b) Matched filter detection response over 6 spatial pixels.

The slit scanning mechanism, which is currently under development, was implemented in a rudimentary form to generate a 19x6 pixel x64 band hyperspectral image. Hypercubes were accumulated at a 1.8Hz frame rate. The matched filter algorithm was implemented in software and applied to the image to produce detection images of a PTFE film transmission target and a 8.18 micron narrowband filter. The results are shown in Figure 9. The image in Figure 9a shows relative positions of PTFE, 400K blackbody and narrowband filter that compose the scene, overlaid by the approximate grid of spatial pixels. Spectra of target and background material radiances, Figure 9b, taken from the hypercube were included in matched filter covariance matrixes.

Results, including a wideband radiance image and matched filter detection maps for the narrow band filter and PTFE film, are shown in Figure 9c. Circles indicate the positions of the two materials in the image. The overlap of key features in the transmission spectra of PTFE and the narrowband filter represents a correlation that can be the cause of confusion for any spectral the detection algorithm. In the case of these matched filters, the correlation was not close enough to pose significant difficulty. As shown in the discussion of Equation 10, matched filter image realizations could be generated 16 times faster than the hyperspectral image, or 0.03s per filter in this case with equivalent SNR.

The wide band radiance image is an approximation formed by summing the results of the matched filter mask pair. The resultant thermal images are observed to be fairly consistent for matched filter pairs of various targets. The narrowband filter, which does not transmit outside its bandpass and is thus relatively cool, does not appear in the wide band image of Figure 9c. The PTFE film is about the same temperature as the blackbody around it and is therefore difficult to distinguish from the background.

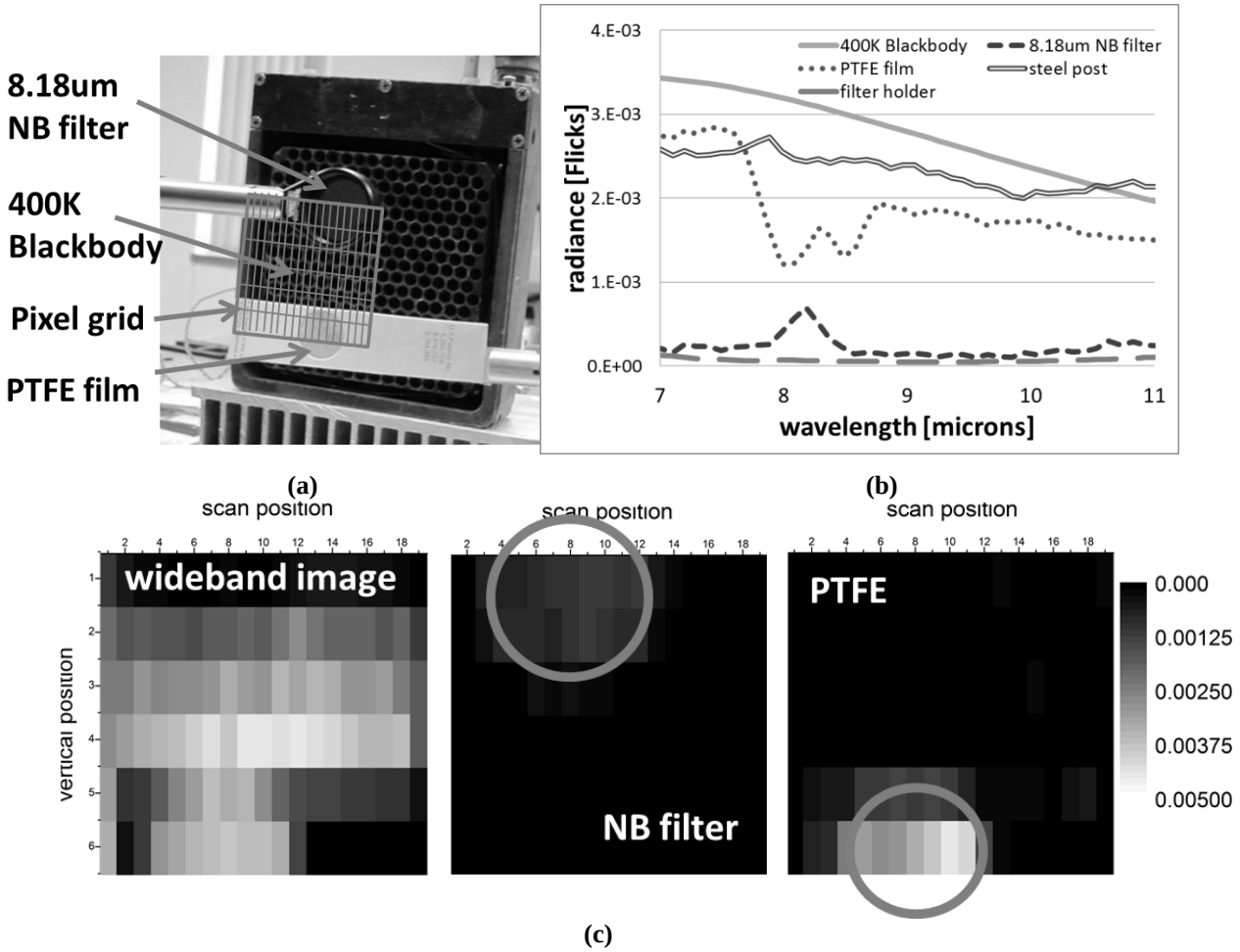

Figure 9. Matched filter detection of PTFE film. a) Scene image showing relative positions of PTFE, 400K blackbody and 8.18 micron narrowband filter against image pixels. b) Spectra of scene target and background material radiances included in covariance matrix. c) Wide-band scene image and detection maps of 8.18micron narrow band filter and PTFE film with circles indicating position of matched filter targets.

3. SUMMARY

The second generation TRACER instrument is currently in the critical design stage. The single detector, combined with a DMD, reduce the size and complexity of components for spectral detection. The hardware matched filter approach provides a fast and relatively simple measurement protocol. Key new components, including the scanning slit, Stirling cooled detector assembly, and customized electronics and firmware, are being developed and tested within the AMS system. Preliminary results of the slit scanning show no loss in spectral imaging performance.

4. ACKNOWLEDGEMENTS

The Authors gratefully acknowledge the Defense Threat Reduction Agency (DTRA), and our technical monitors, Donald Cronce and Morgan Sparks for supporting this work, which was supported under the following contracts: Chemical/Biological Agent Standoff Detection, HDTRA1-05-P-0126 (DTRA), Don Cronce TPOC; TRACER Detection System Phase III BAA, HDTRA3-12-C-0095, Morgan Sparks TPOC. Our thanks to Dr. Thomas Blake of Pacific Northwest National Laboratory for providing independent spectral measurements.

REFERENCES

[1] Goldstein, N., P. Vujkovic-Cvijin, M. Fox, B. Gregor, J. Lee, J. Cline, and S. Adler-Golden, "DMD-based adaptive spectral imagers for hyperspectral imagery and direct detection of spectral signatures," SPIE Vol. 7210,721008 (2009).

[2] Goldstein, N., M. Fox S. Adler-Golden and B. Gregor, "Infrared adaptive spectral imagers for direct detection of spectral signatures and hyperspectral imagery," Proc. SPIE Vol 8618, (2013).

[3] Harwit, M. and N.J.A. Sloane, Hadamard Transform Optics, Academic Press, NY (1979).

[4] Press, W. H., B. P. Flannery, S. A. Teukolsky and W. T. Vetterling, Numerical Recipes in C: The Art of Scientific Computing, Cambridge University Press, pp.408-412 (1992).